

# A Universal Relationship Between Magnetization and the Local Structure in $\text{La}_{1-x}\text{Ca}_x\text{MnO}_3$ ; a Probe of the Magnetization Process

L. Downward<sup>1</sup>, F. Bridges<sup>1</sup>, S. Bushart<sup>1</sup>, J. Neumeier<sup>2</sup> and L. Zhou<sup>3</sup>

<sup>1</sup>Department of Physics, University of California, Santa Cruz, CA 95064, USA

<sup>2</sup>Department of Physics, Montana State University, Bozeman, MT 59717, USA

<sup>3</sup>Stanford Synchrotron Radiation Laboratory, Stanford Linear Accelerator Center, Menlo Park, CA 94025, USA

Received June 26, 2003; accepted November 4, 2003

PACS number: 61.10.Ht

## Abstract

We report X-ray Absorption Fine Structure (XAFS) measurements of the colossal magneto-resistance (CMR) samples  $\text{La}_{0.79}\text{Ca}_{0.21}\text{MnO}_3$  and  $\text{La}_{0.7}\text{Ca}_{0.3}\text{MnO}_3$  at high magnetic fields. For  $T$  near  $T_c$ , the width parameter of the pair distribution function,  $\sigma$ , decreases significantly as the applied magnetic field is increased. For a given magnetization,  $M$ , the decrease in  $\sigma^2$  from the disordered polaron state is the same, irrespective of whether  $M$  was achieved through a change in temperature or the application of an external magnetic field. This universal behavior can be modeled as a quadratic function of magnetization, and suggests a new model for the magnetization process.

In many previous studies,  $\sigma^2$ , the width the Mn-O pair distribution function, decreases rapidly as the temperature ( $T$ ) is lowered below the ferromagnetic transition temperature ( $T_c$ ) for the CMR manganites. This has been attributed to a decrease in the amount of polaron-induced disorder in the magnetized state; similar results have also been observed in neutron pair distribution function (NPDF) analysis studies [1–7]. Furthermore, for several different CMR samples, we have shown that the change in  $\sigma^2$  ( $\Delta\sigma^2$ ) below  $T_c$  can be described by an exponential function of the magnetization, although no theoretical model predicts such behavior [1, 2]. The more extensive study presented here shows that the change  $\Delta\sigma^2$  is only a function of the magnetization  $M$ , irrespective of how  $M$  is produced; it also provides evidence for a new relationship between  $\Delta\sigma^2$  and  $M$ , based on a physical model.

Mn K-edge data were collected on powdered samples of  $\text{La}_{0.79}\text{Ca}_{0.21}\text{MnO}_3$  and  $\text{La}_{0.7}\text{Ca}_{0.3}\text{MnO}_3$  as a function of temperature and magnetic field on beamline 7-2 (Si (111) monochromator crystals) at the Stanford Synchrotron Radiation Laboratory (SSRL). The data were reduced using standard procedures and Fourier transformed to r-space. The r-space Mn-O peak was then fit using the RSFIT program, using standards calculated from FEFF6 [8]. The number of neighbors was constrained to 6, and only the r-space peak position and the width parameter of the pair distribution function,  $\sigma$ , were allowed to vary. ( $S_o^2$  and  $E_o$  were determined at low  $T$  and then held constant for fits to higher temperatures.) Then  $\sigma$  provides a single local structure parameter for comparison with  $M$ . Although one might attempt to model the system as two (or more) Mn-O peaks, there would then be two amplitudes and two  $\sigma$ 's which are partially coupled; a local structure parameter for comparison with  $M$  is then not well defined. For each temperature, independent fits were made to four traces and the average value of  $\sigma$  obtained; the relative errors, the rms fluctuation about the average, is comparable to the symbol size, except where error bars are shown. The absolute errors for  $\sigma^2$ , which depend on  $S_o^2$ , may be of order 10%; they shift the plot vertically.

These first results indicate a significant temperature and magnetic field dependent change in  $\sigma^2$ , near and above  $T_c$  ( $\sim 190$  K for the 21% Ca sample, and  $\sim 260$  K for the 30% Ca Sample) (see Fig. 1 and Fig. 2). At low temperatures, the sample is ordered and  $\sigma^2$  is small while at high temperatures there is a large amount of polaron-induced disorder, as observed previously. Furthermore, there is a field dependent change in  $\sigma^2$ . Near  $T_c$ ,  $\sigma^2$  decreases as the applied field is increased indicating that the application of a magnetic field removes polaron disorder from the sample (see Fig. 1 and Fig. 2).

The change in  $\sigma^2$  is defined as

$$\Delta\sigma^2 = \sigma_T^2 + \sigma_{\text{FP}}^2 + \sigma_{\text{static}}^2 - \sigma_{\text{Mn-O}}^2, \quad (1)$$

where  $\sigma_T^2$  is the thermal contribution calculated from  $\text{CaMnO}_3$  [9],  $\sigma_{\text{static}}^2$  is the excess (above  $\sigma_T^2$ ) contribution at low temperatures,  $\sigma_{\text{Mn-O}}^2$  is calculated from fits to r-space data and is plotted in Fig. 1 and Fig. 2. The difference between  $\sigma_T^2 + \sigma_{\text{static}}^2$  and  $\sigma_{\text{Mn-O}}^2$  at high

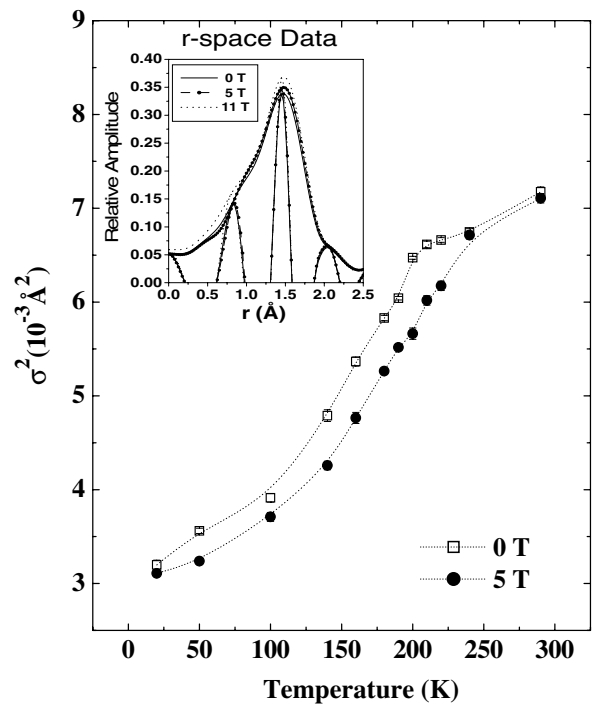


Fig. 1.  $\sigma^2$  vs  $T$  for the Mn-O nearest neighbor peak for the 21% Ca sample. The dotted lines are guides to the eye. The inset shows the corresponding r-space changes in the Mn-O peak at  $T_c$  (190 K) – the amplitude increases ( $\sigma^2$  decreases) with increasing field.

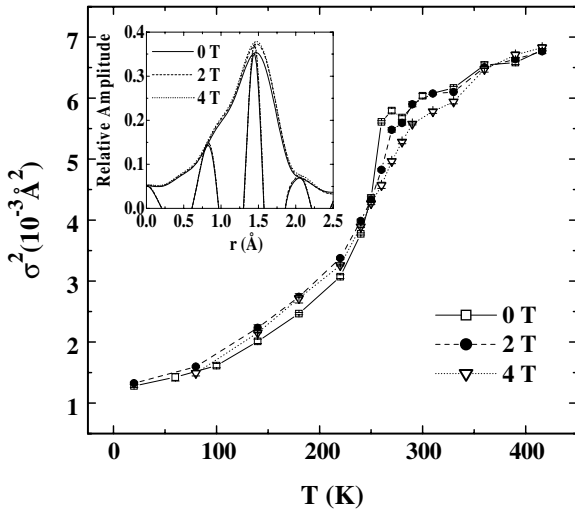


Fig. 2.  $\sigma^2$  vs  $T$  for the Mn-O nearest neighbor peak for the 30% Ca sample. The lines are guides to the eye. The inset shows the corresponding  $r$ -space changes in the Mn-O peak at  $T_c$  (260 K) – the amplitude increases ( $\sigma^2$  decreases) with increasing field.

temperatures is called the full polaronic distortion,  $\sigma_{FP}^2$  in Eq. (1) above [1, 2].

In Fig. 1, we show that for the 21% sample,  $\sigma^2$  decreases as the applied  $B$ -field is increased at constant temperature. A similar dependence on  $B$ -field can be seen for the 30% sample at temperatures near  $T_c$ . However, at lower temperatures for this sample, the change in  $\sigma^2$  is independent of field and  $\Delta\sigma^2$  continues to increase as  $T$  is lowered after the magnetization saturates which occurs at  $\sim 150$  K (compare magnetization data in Fig. 4 inset and Fig. 2).

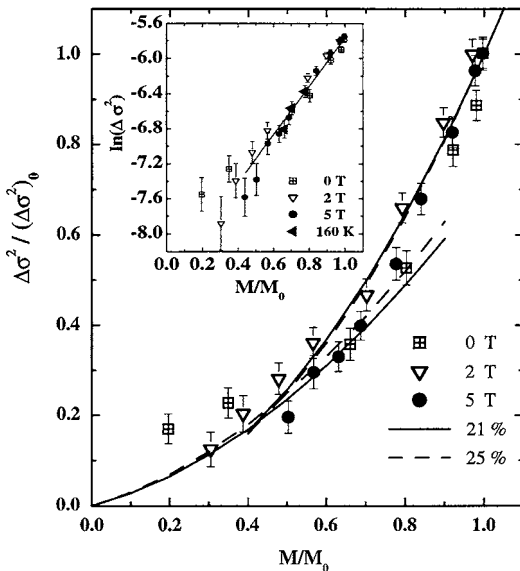


Fig. 3.  $\Delta\sigma^2$  vs relative magnetization for the 21% Ca sample.  $\Delta\sigma^2$  and  $M$  have been normalized to the maximum value for each field.  $\Delta\sigma^2$  is the decrease in  $\sigma^2$  as  $T$  is lowered below  $T_c$  that is attributed to the loss of polaronic distortion. The curves show the theoretical dependence of  $\Delta\sigma^2$  on magnetization given by the quadratic function described in Eq. (2). The inset shows a logarithmic plot of  $\Delta\sigma^2$  vs normalized magnetization; it shows that over this available range in  $M$ , a semi-log plot describes the data quite well. In both plots many of the data points are at a different temperature (i.e. for fixed field, varying  $T$ ). To show more clearly that one can keep  $T$  fixed and vary  $M$  (via a change in  $B$ -field) several points are plotted for  $T = 160$  K. These points lie along the same line in the semi-log plot indicating a universal dependence on  $M$ .

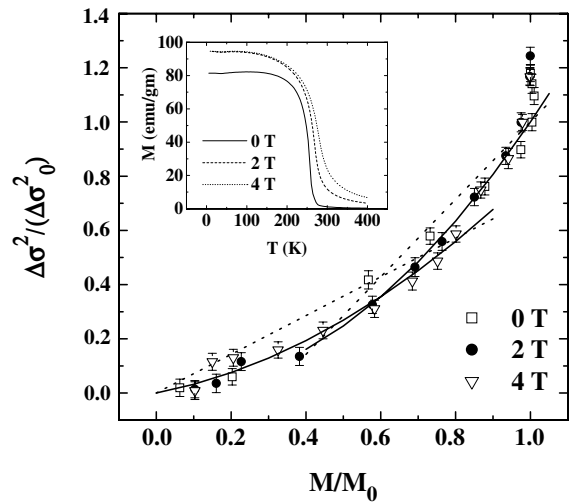


Fig. 4.  $\Delta\sigma^2$  vs relative magnetization for the 30% Ca sample.  $\Delta\sigma^2$  and  $M$  have been normalized to the value at 150 K, when the sample becomes fully magnetized. The curves show the theoretical dependence of  $\Delta\sigma^2$  on magnetization given by the quadratic function described in Eq. (2). The dotted lines show the dependence of a linear fit assuming the distortions are first removed in pairs of distorted  $\text{Mn}^{+3}$  and undistorted  $\text{Mn}^{+4}$  sites, as described in the text. The inset shows the magnetization curve for each field in the plot demonstrating that the sample magnetization is saturated (remains constant) below 150 K. The vertical part near  $M/M_0 = 1$  is evidence that polaron distortions are continuing to be removed after the sample has become fully magnetized.

The observed changes in  $\Delta\sigma^2$  can be modeled by either an exponential function or a polynomial function of magnetization where there are regions of differing behavior see Fig. 3 and Fig. 4. A semi-log plot for the 30% sample is similar to the inset for the 21% sample. The magnetization has been normalized to the saturation value while  $\Delta\sigma^2$  has been normalized to the value at which the sample becomes fully magnetized; this occurs at the lowest temperature for the 21% sample, but at  $\sim 150$  K for the 30% sample. The relatively slow change in  $\Delta\sigma^2$  at low  $M$  indicates that the lowest-distortion sites must become magnetized first. Since the “ $\text{Mn}^{+4}$ ” site is thought to be essentially undistorted, the magnetization process may proceed in pairs – an undistorted “ $\text{Mn}^{+4}$ ” site and a distorted “ $\text{Mn}^{+3}$ ” site; this allows an electron to hop back and forth between two Mn sites as required in the double exchange model but only required that one of the distorted sites become undistorted. Once all the “ $\text{Mn}^{+4}$ ” sites become magnetized (60% of the sample is magnetized for the 30% sample), further increases in  $M$  require that every additional Mn site must become undistorted. Since a significant cluster must be magnetized in ferromagnetic systems it is likely that the magnetized clusters form filaments through the sample and the magnetic and non-magnetic regions are intertwined. For the 30% sample, the vertical part near  $M/M_0 = 1$  in Fig. 4 is evidence that polaron distortions are continuing to be removed after the sample has become fully magnetized, which indicates that the Mn sites can be magnetized but still have a small local distortion. A possible explanation is that the polarons are still partially localized at 150 K. Only at the lowest temperatures are the polarons essentially delocalized.

The magnetization process described above can be described by the following model. Let the smallest polaron distortions removed be  $\alpha_0$ , and assume that there is a distribution of distortions that are removed with the largest distortions removed when  $M \sim M_0$ . The distortion that is removed at various states of magnetization ( $f$  is the fractional magnetization ( $M/M_0$ )), can be

described as  $\alpha = \alpha_o(1 + \gamma f)$ , where  $\gamma$  is a measure of the range of distortions. Below the critical value of  $f$  (twice the Calcium concentration,  $2x$ ) the distortion removed per pair is only  $\alpha$ ; above this value of  $f$  the distortion removed per pair is  $2\alpha$ . This leads to the following normalized expressions which were used to fit the  $\Delta\sigma^2$  data:

$$\frac{\Delta\sigma^2}{\Delta\sigma_0^2} = \begin{cases} \frac{1}{2}Af(1 + \gamma f) & \text{for } f \leq f', \\ \frac{1}{2}Af'(1 + \gamma f') + A(f - f')(1 + \gamma f) & \text{for } f > f', \end{cases} \quad (2)$$

where  $f'$  is the critical value of  $f$  (twice the Calcium concentration,  $2x$ ), and  $A$  is a normalization constant equal to  $\frac{1}{\Delta\sigma_0^2}$ , where  $\Delta\sigma_0^2$  is value of  $\Delta\sigma^2$  when  $f = 1$ .  $\gamma = 2$  gives good agreement with the data in Figs. 3 and 4.

We have extended our previous results [1, 2] to show that the relationship between  $\sigma^2$  and magnetization, is more universal. Changing the sample magnetization by either varying the applied field or varying the temperature produces similar changes in  $\sigma^2$ . Further analysis needs to be done to investigate the full nature of this relationship.

## Acknowledgments

The experiments were carried out under NSF grant DMR0301971 and were performed at SSRL, which is operated by the U.S. DOE, Division of Chemical Sciences, and by the NIH, Biomedical Resource Technology Program, Division of Research Resources.

## References

1. Booth, C. H. *et al.*, Phys. Rev. Lett. **80**, 853 (1998).
2. Booth, C. H. *et al.*, Phys. Rev. B **57**, 10440 (1998).
3. Billinge, S. J. L., DiFrancesco, R. G., Kwei, G. H., Neumeier, J. J. and Thompson, J. D., Phys. Rev. Lett. **77**, 715 (1996).
4. Cao, D., Bridges, F., Worledge, D. C., Booth, C. H. and Geballe, T., Phys. Rev. B **61**, 11373 (2000).
5. Cao, D., Bridges, F., Booth, C. H. and Neumeier, J. J., Phys. Rev. B **62**, 8954 (2000).
6. Subías, G., García, J., Proietti, M. G. and Blasco, J., Phys. Rev. B **56**, 8183 (1997).
7. Tyson, T. A. *et al.*, Phys. Rev. B **53**, 13985 (1996).
8. Zabinsky, S. I., Rehr, J. J., Ankudinov, A., Albers, R. C. and Eller, M. J., Phys. Rev. B **52**, 2995 (1995).
9. Cao, D. *et al.*, Phys. Rev. B **64**, 184409 (2001).